Coherent wave patterns sustained by a localized inhomogeneity in an excitable medium

Bing-Wei Li,[1] Hong Zhang,[1,*] He-Ping Ying,[1,†] and Gang Hu[2,‡]
[1]*Zhejiang Institute of Modern Physics and Department of Physics, Zhejiang University, Hangzhou 310027, China*
[2]*Department of Physics, and The Beijing-Hong Kong-Singapore Joint Centre for Nonlinear and Complex Systems (Beijing), Beijing Normal University, Beijing 100875, China*

(Received 26 September 2008; revised manuscript received 19 December 2008; published 26 February 2009)

The influence of a localized inhomogeneity (oscillatory or stationary) on spatiotemporal chaotic state in an excitable reaction-diffusion system is investigated. We find that various coherent wave patterns, such as spiral waves (including multiarmed) and target wave patterns are able to be created by the inhomogeneity from the chaotic state. Due to the growth of these coherent wave patterns, the previously existing turbulent waves in the absence of inhomogeneity are suppressed. At last, the whole system is entrained by the coherent wave patterns. Closer investigations indicate that the possible mechanisms underlying the inhomogeneity sustained coherent wave patterns seem quite different for oscillatory and stationary inhomogeneities.

DOI: 10.1103/PhysRevE.79.026220 PACS number(s): 89.75.Kd, 47.54.−r, 82.40.Ck

I. INTRODUCTION

Spatially distributed active systems, modeled by a set of reaction-diffusion (RD) equations, are able to sustain a wide class of coherent wave patterns [1,2]. Two examples commonly observed in physical, chemical, or biological systems are target wave and spiral wave patterns. These wave patterns have received much attention during the last thirty years because of their interesting nonlinear dynamics and their potential applications in various biological or physiological systems [2]. In addition to these coherent wave patterns, spatiotemporal chaotic wave patterns (sometimes referred to as "chemical turbulence") have also been encountered in the experiments, such as the Belousov-Zhabotinsky (BZ) reaction [3], CO oxidation on Pt(110) [4], and in numerical simulations [5]. Taming spatiotemporal chaotic patterns in spatially extended systems has been achieved so far using various strategies, e.g., global [4,6,7] and local methods [8–18].

In realistic systems such as chemical reactions [19,20] or biological tissues [21,22], inhomogeneities are found to be fairly ubiquitous. Both numerical simulations and experimental results show that the roles they play in spatiotemporal dynamics are quite important. For example, a meandering spiral wave could be forced to rigidly rotate if we introduce an unexcited inhomogeneity closely to the spiral tip [23]; a localized inhomogeneity can lead to attracting or repelling of a spiral wave in excitable media [24,25]. Once a spiral is pinned, its period linearly depends on the radius of the inhomogeneity and is generally larger than that of the free stable spiral [26]. More interestingly, Pumir *et al.* [27] recently showed that new ordered waves (e.g., target waves) can be triggered from the inhomogeneities by applying the electric field and previously existing spatiotemporal chaotic waves give way to these new ordered waves. This approach opens up a way to control spatiotemporal chaotic waves in excitable media. Additionally, in oscillatory media (e.g., the complex Ginzburg-Landau system), both target wave patterns and spiral wave patterns could be created by introducing a localized inhomogeneity in spiral turbulence. Eventually, the system will be driven by the coherent wave patterns [11].

The effect of a localized inhomogeneity on spiral waves in excitable media has been studied by many authors, however, we note that most of them concentrate on its influence on a single spiral wave. To our best knowledge, information about the effect of a localized inhomogeneity on spatiotemporal chaotic waves in excitable media is still less and poorly known [28,29]. In this paper, we will show that coherent wave patterns, including spiral waves with single-or multiple-armed as well as target wave patterns could be promoted and then grown around the introduced inhomogeneity. Due to the growth of the coherent wave patterns, the spatiotemporal chaotic waves can be suppressed by them and finally the system remains in a coherent state. We also discuss the possible mechanisms underlying the emergence of these kinds of coherent structures.

II. THE MODEL AND RESULTS

To study the influences of a localized inhomogeneity on spatiotemporal chaotic dynamics, a modified FitzHugh-Nagumo–type equation is employed throughout this paper. The equation reads [5]

$$\frac{\partial u}{\partial t} = \frac{1}{\epsilon}u(1-u)\left(u-\frac{v+b}{a}\right)+D\nabla^2 u, \tag{1}$$

$$\frac{\partial v}{\partial t} = g(u) - v, \tag{2}$$

where $g(u)=0$ when $0\leqslant u<1/3$; $g(u)=1-6.75u(1-u)^2$ when $1/3\leqslant u\leqslant 1$; $g(u)=1$ when $u>1$. ϵ represents a time ratio between activator u and inhibitor v and a,b are two other parameters of the system. D is a diffusion coefficient of u. The above equation actually is a reduced version to describe the surface reaction of CO oxidation on Pt(110) [30].

*Author to whom correspondence should be addressed. hongzhang@zju.edu.cn, hzhang@zimp.zju.edu.cn
†hpying@zimp.zju.edu.cn
‡ganghu@bnu.edu.cn

Depending on the parameters a and b, the system can experience rich dynamics such as excitable or oscillatory behavior. Specifically, the system undergoes saddle-node bifurcation at $b=0$, and it is in the oscillatory regime for negative b while excitable for positive b with $a<b+1$ [5]. It has been interestingly noted that for certain parameters in the excitable regime, e.g., $a=0.84$, $b=0.07$, the transition from spiral wave patterns to spatiotemporal chaotic state associated with spiral turbulence could be observed [5] as we vary the excitability ϵ to beyond the critical value $\epsilon_c=0.07$.

Using microelectronics fabrication techniques [31–34], one can construct or design the composite media by coupling of a pure Pt(110) with a small partial of other metals (e.g., Au, Pd, Rh, etc.). From another point of view, this small region imposed by other metals can be regarded as a kind of inhomogeneities or defects. As pointed out in Ref. [33], this kind of composite media (or media with inhomogeneities in other words) can be mimicked in the model by writing b as a spatial dependence $b(\mathbf{r})$. For simplicity, a localized inhomogeneity, throughout our study, is hence introduced in a following manner, similar to the one in Ref. [33,34]

$$b(r)=\begin{cases} b_1, & \text{for } r\leq r_0, \\ b_2, & \text{for } r>r_0, \end{cases} \tag{3}$$

where $r=\sqrt{(x-x_0)^2+(y-y_0)^2}$ and (x_0,y_0) denotes center coordinates of the inhomogeneity. r_0 is the radius of the inhomogeneity and it is much smaller than the scale of the whole studied system. If $b_1=b_2$, the system is uniform.

For Eqs. (1) and (2), it is found that different values of b denote different dynamics for the zero-dimensional $(D=0)$ system for the fixed parameters a and ϵ, e.g., $a=0.84$ and $\epsilon=0.085$. That can be reflected by the property of the fixed point between two nullclines as shown in Figs. 1(a) and 1(b), corresponding to two typical cases $b=-0.10$ and $b=-0.30$, respectively. In these two plots, the dashed lines denote $\dot{u}=0$ and the solid line denotes $\dot{v}=0$, respectively. Generally, for instance, if $-0.16<b<0$, there is only one fixed point and it is found unstable. In this case, the system demonstrates a limit cycle behavior provided that an initial perturbation is applied around the fixed point, as shown in Fig. 1(c); if $b<-0.16$, there is at least a fixed point, e.g., $(u,v)=(1.0,1.0)$ and only this fixed point is stable (in a very narrow parameter regime, i.e., $-0.19<b<-0.16$, more than one fixed point could exist). Under this situation, the system will relax to this state from the small perturbed initial condition, as shown in Fig. 1(d). (A sufficiently large perturbation, e.g., beyond the middle u nullclines, would make a large excursion before it returns to the fixed point.) Hence, a local change of b will locally vary the dynamics behavior of the system. In the following, we refer the inhomogeneity to be oscillatory if $-0.16<b_1<0$ and be stationary if $b_1<-0.16$. The medium is excitable $(b_2=0.07)$ and depending on the value of b_1, the inhomogeneity is either oscillatory or stationary.

The aim of this work is to study how a local change of b (or localized inhomogeneity) affects the whole chaotic dynamics, particularly in generating coherent structures. To numerically integrate Eqs. (1) and (2) explicit Euler method

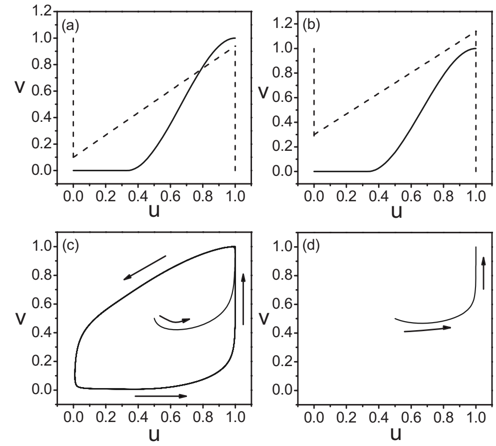

FIG. 1. (a), (b) Nullclines $\dot{u}=0$ (dashed lines) and $\dot{v}=0$ (solid line) of Eqs. (1) and (2). The only change induced by b is the middle branch of the u nullcline: (a) $b=-0.10$ and (b) $b=-0.30$. Different values of b here denote the different fixed points between two nullclines $(\dot{u}=0,\dot{v}=0)$ and thus describe distinct dynamics of zero-dimensional system (1) and (2). (c), (d) Two different trajectories, corresponding to $b=-0.10$ (c) and $b=-0.30$ (d) in phase space (u,v) from the uniformly perturbed initial state [e.g., $(u,v)=(0.5,0.5)$]. One finds that for $b=-0.10$, the system exhibits limit cycle behaviors and that for $b=-0.30$ it relaxes to stationary state $(u,v)=(1.0,1.0)$. Arrows appeared in figures of (c) and (d) mean the direction followed by the trajectories. The system parameters are $\epsilon=0.085$, $a=0.84$, $D=0$.

with the spatial step $\Delta x=\Delta y=0.3906$ and time step $\Delta t=0.02$ is employed. Main results are also checked by smaller time step. No-flux boundary conditions are considered. If no other statements are specified, we use the following parameters: the size of system is $L_x=L_y=100$, consisting of 256×256 grid points; we fix $a=0.84$, $b_2=0.07$, $D=1$ and take $\epsilon=0.085$. In the following study, we only focus on the case that the value of b_1 is negative.

We first examine the possible influences of an inhomogeneity, which belongs to the oscillatory regime, i.e., $b_1\in(-0.16,0.0)$, on the spatiotemporal chaotic state. An interesting result is illustrated in Fig. 2. Figure 2(a) is an initial condition showing chaotic waves resulted from a spiral breakup for $\epsilon=0.085$. If the system is uniform, namely, $b_1=b_2=0.07$, it consists of an ensemble of locally interacting spiral waves whose annihilation and generation are repeated, and the configuration remains similar. However, this kind of spatiotemporal chaotic configuration could be altered to a coherent structure, i.e., a spiral wave pattern, when we introduce a localized inhomogeneity, e.g., $b_1=-0.085$. The inhomogeneity is denoted by the circular region in each snapshot of Fig. 2. Evidently as seen in snapshots in Fig. 2, a spiral wave begins to grow around the location of the inhomogeneity [see Figs. 2(b) and 2(c)], after a transient period. Finally, the initial spiral turbulent waves are suppressed by the growing spiral wave and the whole system is dominated by it [see Fig. 2(d)]. To summarize this evolution process, a space-time plot is also displayed in Fig. 2(e). In this figure, T_1 denotes the time from that we switch on the inhomogeneity to that the spiral begins to grow; T_2 denotes the time from that the spiral begins to grow until to that the fully developed

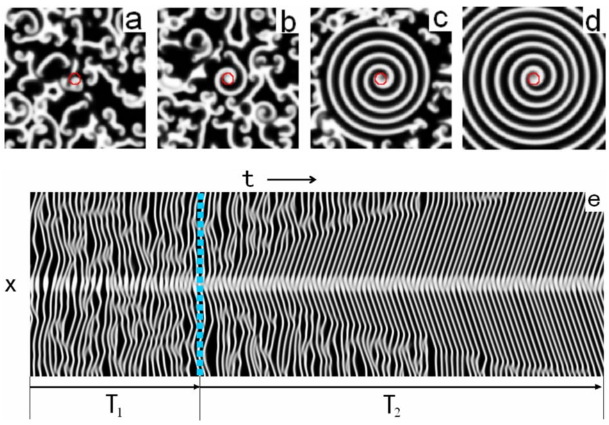

FIG. 2. (Color online) (a)–(d) A typical process of spiral wave pattern formation induced by a localized inhomogeneity, e.g., $b_1 = -0.085$. The circular region ($r \leqslant r_0 = 10.0$) denotes the introduced inhomogeneity. (e) Corresponding space-time plot at $y=50$. The dashed line denotes the time when a spiral begins to grow. T_1 denotes the time from that we switch on the inhomogeneity to that the spiral begins to grow. This time depends on the initial conditions (or the location where we introduce the inhomogeneity). T_2 denotes the time from that the spiral begins to grow until to that the fully developed one is formed. This time keeps similar if the parameters are the same. The system is 100×100, consisting of 256×256 grid points. The space step and time step are $\Delta x = \Delta y = 0.3906$ and $\Delta t = 0.02$, respectively.

one is formed. It is worth mentioning that it will take some time (i.e., $T_1 + T_2$) until an inhomogeneity will be able to entrain the system. This time depends on the initial conditions (or the location where we introduce the inhomogeneity) and parameters. In our simulations, in most cases, we find it takes the time about 2000 time units and in a few cases it needs longer time. All results throughout this paper are able to be observed in less than 5000 time units.

Whether a coherent wave pattern, i.e., a spiral wave, can be generated or not mainly depends on the values of b_1. To find out which values of b_1 in the oscillatory regime [i.e., $b_1 \in (-0.16, 0.0)$] could induce and maintain the coherent wave pattern, we perform a large number of numerical experiments (about 81 cases using different initial conditions and radii of the inhomogeneity for each value b_1) for $\epsilon = 0.085$. We find the values of b_1 should be chosen suitably if we want to create the spiral wave pattern from the turbulent state. Specifically, to possibly generate the spiral wave pattern, the values of b_1 are required into a quite narrow region $b_1 \in [-0.12, -0.08]$ (we discretize the region for b_1 with a step $\Delta b_1 = 0.01$ in practical simulations) and no coherent wave patterns are observed if b_1 is beyond this region, i.e., $b_1 \in (-0.16, -0.12)$ or $b_1 \in (-0.08, 0.0)$. Yet, this region of b_1 that can induce the coherent spiral pattern might vary for different ϵ. For example, we find to give a transition from chaotic state to coherent wave patterns, the region for b_1 could be extended to $b_1 \in [-0.12, -0.01]$ for $\epsilon = 0.071$. The possible reasons underlying this kind of difference will be discussed later.

As we further decrease the value of b_1, the inhomogeneity would fall into the stationary regime (i.e., $b_1 < -0.16$). In this

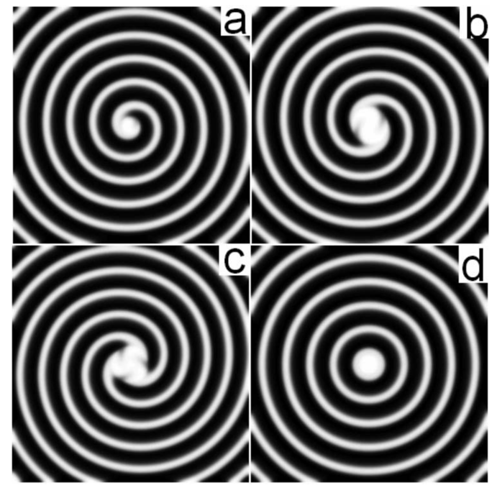

FIG. 3. Various coherent wave patterns induced by the stationary inhomogeneity. (a) $b_1 = -0.26$, one-armed spiral wave; (b) $b_1 = -0.21$, two-armed spiral wave; (c) $b_1 = -0.20$, three-armed spiral; and (d) $b_1 = -0.365$, target waves. The radius of the inhomogeneity is $r_0 = 10.0$ in (a), (d) and $r_0 = 20.0$ in (b), (c).

case, the inner region of the inhomogeneity almost remains in the stationary state, i.e., $(u, v) = (1.0, 1.0)$. Under this situation, in addition to one-armed spiral waves, other coherent wave patterns such as multiarmed spiral wave patterns and even target wave patterns are interestingly observed. These examples are depicted in Fig. 3. Figure 3(a) is one-armed spiral; Figs. 3(b) and 3(c) describe two-armed and three-armed spiral wave patterns, respectively; a typical target wave pattern emerges in Fig. 3(d). By measuring the frequencies of multiarmed spirals, we find that their frequencies are generally larger than the frequency of the single-armed spiral.

To give rise to multiarmed spiral wave patterns, our intensive simulations indicate that the radius of the inhomogeneity should not be too small. To be concrete, no two-armed spiral patterns are observed when $r_0 \leqslant 10.0$ and no three-armed when $r_0 \leqslant 18.0$ in our simulations. This phenomenon may be understood intuitively. If the radius of the inhomogeneity is larger, there are more opportunities for small localized spirals to touch the edge of the inhomogeneity. Once some spirals are attracted to the inhomogeneity, then they may grow and rotate together around the introduced inhomogeneity. In this sense, one of possible factors to affect the selection of coherent wave patterns, single-armed spiral patterns, or multiarmed spiral patterns, is related to the initial configuration of u and v around the inhomogeneity if r_0 is sufficient large.

To induce and sustain coherent spiral wave patterns, we note that no particular spiral seed is required, which is analogous to our recent study in the framework of the complex Ginzburg-Landau equation (CGLE) [11]. This evidence, to some extent, indicates that the location where we introduce the inhomogeneity and the time when we switch on the inhomogeneity (i.e., initial conditions) are not very crucial for generating coherent wave patterns. This is indeed confirmed by our numerical simulations. As an illustrative example, we introduce some (e.g., five) inhomogeneities with the exactly

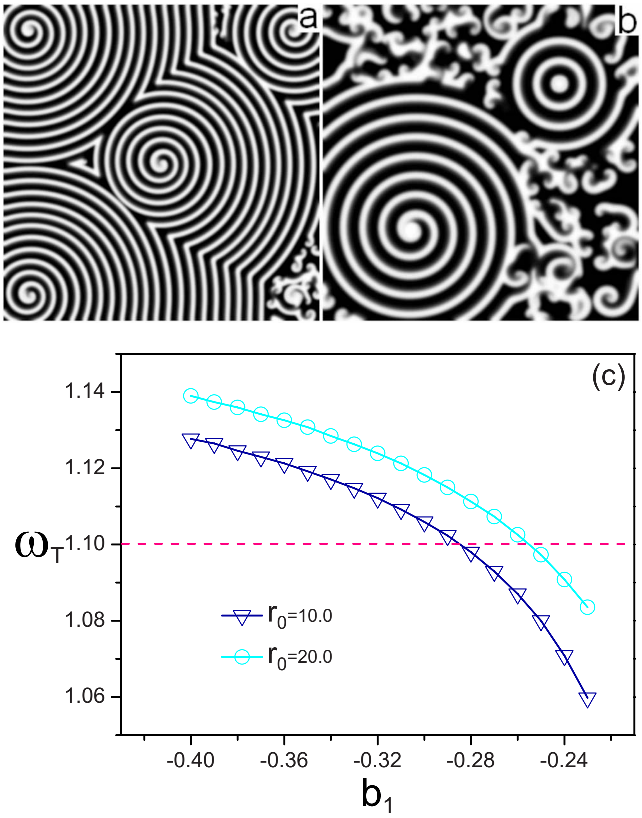

FIG. 4. (Color online) (a) Effect of the inhomogeneity location on generating spiral wave patterns. In this system, we introduce five inhomogeneities with the same properties, e.g., $r_0=10.0$ and $b_1=-0.09$. For simplicity, we locate them on the two straight lines. In the asymptotic state, we find four coherent spiral wave patterns coexist and one (in right bottom corner) is suppressed. This result to some extent implies that formation of coherent spiral wave patterns hardly depends on its locations of the introduced inhomogeneity. The system is composed of 600×600 grid points. (b) An example of two types of wave patterns, say spiral waves and target waves, induced by two inhomogeneities with the exactly same properties $r_0=10.0$ and $b_1=-0.325$. In the asymptotic sate, target waves are suppressed by spiral waves. The system consists of 400×400 grid points. (c) Dependence of the frequency of target waves, denoted by ω_T, on b_1 for $r_0=10.0$ (triangles) and $r_0=20.0$ (circles). The dashed line denotes the background frequency $\omega_0\approx1.10$ of turbulent state for $\epsilon=0.085$, $a=0.84$, $b=0.07$ of Eqs. (1) and (2).

same properties, i.e., $b_1=-0.09$ and $r_0=10.0$, but in different locations in a much larger system. The location of the inhomogeneity is arbitrarily chosen without any intention. For simplicity, we locate them on the two straight lines. Figure 4(a) shows the result. As one finds, spiral wave patterns are able to grow around the location where the inhomogeneity is introduced.

We would like to point out that the case in the same system with several inhomogeneities in different locations at the same time differs from the situation that we put only one inhomogeneity in the system in each simulation. This is because the waves elicited by the inhomogeneities in the system will interact with each other. Even though the grow speed ($\propto 1/T_2$) is similar for the exactly same inhomogeneity, the transient time [i.e., T_1 in Fig. 2(e)] may be different. For example, a spiral wave around some locations grows slower [see the small spiral in right bottom corner in Fig. 4(a)] than the ones around other locations. As a result, this one will be suppressed by other ones before it begins to grow. In the asymptotic state, we find only four spiral waves can coexist. We have also tested with different initial conditions and one inhomogeneity, and found that the results do not depend sensitively on them. These results seem a little bit different from those shown in Ref. [29] where the authors demonstrated that spatiotemporal chaotic dynamics relies sensitively on the inhomogeneity in a mathematical models of ventricular tissue. For instance, even a slight change of the location of the inhomogeneity, the resulted dynamics changes drastically [29].

For the stationary case (i.e., $b_1<-0.16$), formation of coherent wave patterns are also insensitively dependent of locations of the inhomogeneity and initial conditions. More interestingly, differing from the oscillatory case [i.e., $b_1\in(-0.16,0)$], where only spiral wave patterns (i.e., $b_1\in[-0.12,-0.08]$) could be induced, we find both spiral wave and target wave patterns are possible to be induced even by the exactly same inhomogeneity. Which kind of coherent wave pattern, spiral or target, is finally selected may depend on the location of the inhomogeneity and initial conditions. To show this point, we introduce two inhomogeneities, as an example, in different positions but with exactly the same properties. We find both spiral and target wave patterns can be generated [see Fig. 4(b)]. In the asymptotic state, the target waves will be suppressed by the spiral waves because of $\omega_s>\omega_T$.

The rational behind the fact that the exactly same inhomogeneity selects different coherent wave patterns is related to the frequency. To show this point, we measure the frequency of target waves for different values of b_1. To do this, we use the uniform initial conditions and introduce the inhomogeneity in the system. Under this situation, the inhomogeneity plays a role of a pacemaker and a target wave would appear. When it is fully developed, and then we record the time series of the variable u for any grid point far from the pacemaker (the center of the inhomogeneity). According to this time series, we can get the frequency (or period) of the target wave. In Fig. 4(c), we give the dependence of the frequency of the target wave on b_1 for $r_0=10.0$ (triangles) and $r_0=20.0$ (circles). From this figure, we find that its frequency is over the background frequency [dashed line, $\omega_0\approx1.10$, obtained by the fast Fourier transform (FFT) method] of the chaotic waves once b_1 is smaller than a critical value b_{1c} (e.g., $b_{1c}\approx-0.28$ for $r_0=10.0$).

According to the wave competition rule in excitable media [35], on one hand, this fact indicates that the target wave is possible to be created from the turbulent state because its frequency is larger than the background frequency. On the other hand, spiral waves do not immediately grow as we introduced the inhomogeneity. In general, it would take some time [i.e., T_1 illustrated in Fig. 2(e)] that depends on the initial conditions. Therefore, creation of target waves from spiral turbulent waves is greatly possible if new target waves begin to emit from the inhomogeneity before a small spiral is stably attached to it and begins to grow. This is because once new target waves are initialized at the inhomogeneity, they are able to sweep the turbulent waves due to the frequency relation and keep spiral tips far away from the inhomogeneity. Then there is no chance for spiral tips to come again closely to the inhomogeneity. Finally the stable target waves rather than the spiral waves survive. For $b_1 > b_{1c}$, almost no target waves are observed because they are suppressed by the turbulent waves and under this situation only coherent spiral wave patterns would emerge [see Fig. 4(a) for example].

The radius of the inhomogeneity would affect the frequency of the resulted target wave [see Fig. 4(c)]. From Fig. 4(c), it is found that the frequency increases as we increase the radius for the same b_1. Actually, the frequency dependence on the radius of the inhomogeneity is quite similar to the case of oscillatory media [36]. Due to this dependence, the critical value b_{1c} is also changed. For example, $b_{1c} \approx -0.255$ for $r_0 = 20.0$.

Both oscillatory and stationary inhomogeneities, as we found, are able to induce and sustain spiral wave patterns. Yet a closer examination indicates that the characteristics of the spiral induced by these two types of the inhomogeneity seem a little different. These differences are reflected by the following facts.

We refer the first point to the tip orbit. On one hand, for the stationary inhomogeneity sustained spiral, as we note that, the motion of its tip always follows the edge of the inhomogeneity; but for the oscillatory inhomogeneity sustained spiral, in some situations, the motion of its tip is limited to the inner region of the inhomogeneity. This fact, to some extent, can be reflected by the dependence of average radius of the tip orbit, denoted by $\langle r \rangle$, on the radius of the inhomogeneity [see Fig. 5(a)]. In the case of stationary inhomogeneity, $\langle r \rangle$ is almost equal to the radius of the inhomogeneity but in some situations for the oscillatory case, $\langle r \rangle$ is smaller than r_0. On the other hand, we measure the dependence of frequency on r_0 for $b_1 = -0.255$ (triangles) and $b_1 = -0.275$ (circles) [see Fig. 5(b)]. For the stationary inhomogeneity sustained spiral, we find the frequency decreases as we increase r_0 for a given b_1. [The dependence of the spiral frequency on b_1 is similar to Fig. 4(c).] These features indicate that the formation of spiral waves sustained by the stationary inhomogeneity may result from an anchoringlike effect [26]. However, for the oscillatory inhomogeneity sustained spiral, its frequency dependence on r_0 is nonmonotonic and seems a little complex [see the inset in Fig. 5(b)].

Another point we would like to mention is the stability of the resulted spiral waves. To be concrete, stationary inhomogeneity sustained spirals always rigidly rotate, but most of oscillatory inhomogeneity sustained spirals demonstrate meandering behavior. This difference could be seen by performing the power spectra analysis, as shown in Figs. 5(c) and 5(d). In the power spectra of the rigidly rotating spiral, there is only one fundamental frequency [the maximal peak in Fig. 5(d)], but in the power spectra of the meandering spiral there are two fundamental frequencies (i.e., ω_1 and ω_2) and others are linear combinations of ω_1 and ω_2 [see Fig. 5(c)].

The differences discussed above suggest that it seems necessary to distinguish the two different types of the inhomogeneity to understand better the formation of coherent wave patterns, particularly spiral waves. For the oscillatory case, let us first examine what kinds of wave patterns the

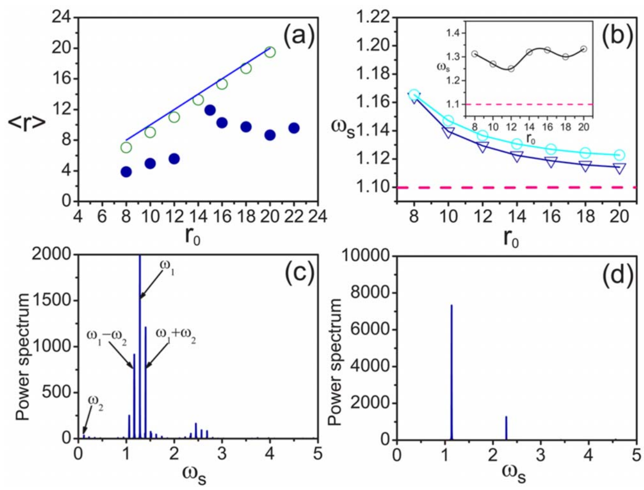

FIG. 5. (Color online) (a) Dependence of average radius $\langle r \rangle$ of the tip orbit for two different inhomogeneities sustained spirals: $b_1 = -0.095$, $\epsilon = 0.071$ (full circles) and $b_1 = -0.255$, $\epsilon = 0.085$ (open circles). The spiral tip position is identified by maximizing the vector product $|\nabla u \times \nabla v|$. The solid line indicates $\langle r \rangle = r_0$. (b) Dependence of the frequency of spiral waves on the radius r_0 of the stationary inhomogeneity for $b_1 = -0.255$ (triangles) and $b_1 = -0.275$ (circles). The inset plot in this figure shows the dependence of the frequency for spiral waves on r_0 for the oscillatory case $(b_1 = -0.09)$. The dashed line denotes the background frequency of the turbulent waves. (c) and (d) Two typical kinds of power spectrum of one site for spiral waves induced by two different inhomogeneities, (c) $b_1 = -0.085$ and (d) $b_1 = -0.255$ for $\epsilon = 0.085$. In the plot (c), there are two fundamental frequencies, i.e., ω_1 and ω_2. ω_1 is the primary frequency of stable spiral waves and ω_2 is the secondary frequency caused by the Hopf bifurcation. Other frequencies are linear combinations of them. In the plot (d), only one fundamental frequency (i.e., the maximal peak) exists.

uniform system [i.e., $b_1 = b_2 = b \in (-0.16, 0.0)$] can support. To this end, we numerically calculate the phase portrait for $b - \epsilon$ of the uniform system, as illustrated in Fig. 6. There are three regions: the gray region denotes that the medium itself is able to support stable spiral waves in this parameter region and in other two regions, only the breaking waves could be observed. For example, for $\epsilon = 0.085$ and $a = 0.84$, stable spiral waves can be observed in the region $[-0.12, -0.07]$ and turbulent waves (or breaking waves) in the remaining regions, i.e., $(-0.16, -0.12)$ and $(-0.07, 0.0)$.

In this phase portrait, we also give the possible values of b_1 (full circles) that could generate spiral wave patterns from the chaotic state for $\epsilon = 0.071$ and $\epsilon = 0.085$, as examples. Open circles denote that no coherent wave patterns are observed in our simulations. One can see that to create spirals from a chaotic waves, the value b_1 is required into the gray region. This means that to induce and sustain a spiral wave pattern, the local inhomogeneity region itself should have an ability to support spiral waves. In this sense, formation of spiral waves from a chaotic state may result from a local survival of the small spiral in the small inhomogeneity region. From this point of view, understanding the formation of spiral waves in the case of oscillatory inhomogeneity could be intuitively: when a small spiral either initially exists or comes into the inhomogeneity region in later time, it is pos-

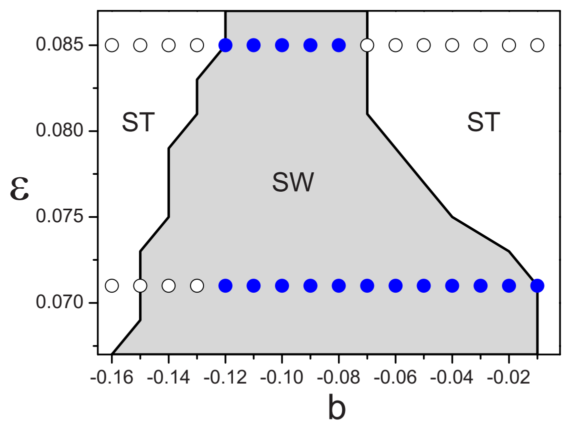

FIG. 6. (Color online) Phase portrait for $b-\epsilon$ for uniform system (1) and (2). One finds that there are three regions. The shade regions denote stable spiral waves (SWs). The other two regions denote spiral turbulence (ST). The full circles represents the chosen value of $b_1=b$ could induce coherent spiral wave patterns from chaotic state for fixed $a=0.84$, $b_2=0.07$. The open circles denotes the region where no coherent wave patterns are observed in our simulations. To numerically obtain this phase portrait, we use initially cross-gradient value of u and v [30].

sible to survive and grow since this inhomogeneity region itself can support stable spiral waves. Once the frequency of the inhomogeneity sustained spiral is larger than the background frequency of turbulent waves, it may grow further and sweep the turbulent waves close to it. Eventually, the surviving spiral dominates the system.

Considering that the spiral finally dominating the system is a local survival of the one in the inhomogeneity region, a reasonable assumption is that its tip should be limited into the inhomogeneity region. This assumption is coincident with previous results. For instance, $\langle r \rangle$ is smaller than the radius of the oscillatory inhomogeneity [refer to Fig. 5(a)]. From Fig. 6, we also find the gray region that could support stable spiral waves varies for different values of ϵ. This evidence may explain why the region of b_1 that is able to induce spiral patterns is changed for different parameters ϵ as we pointed out previously.

For the case of the inhomogeneity in the stationary regime, it is found that the inhomogeneity itself can not sustain the spiral waves (even turbulent waves) anymore. We mean that if the system is uniform, from the initial conditions used in Fig. 6, the whole system will relax to a stationary state and no waves can be observed. For this case, we would like to refer the creation of spiral patterns from the chaotic state to an anchoringlike effect, as reflected by Figs. 5(a), 5(b), and 5(d). If a small spiral wave is attracted by the inhomogeneity, its frequency will be affected by it. This local perturbation induced frequency shift of chemical waves has been considered previously [11,37,38]. If the frequency of the spiral pinned to the inhomogeneity is larger than the background frequency of spatiotemporal chaotic state, a coherent spiral pattern could grow and the system is finally dominated by it (see Figs. 3 and 4).

III. DISCUSSION AND CONCLUSION

So far, we have shown that a small localized inhomogeneity can induce and maintain coherent wave patterns in an excitable medium. These coherent patterns include spiral waves and target waves. In this sense, the results presented in this paper and our previous work [11] share the common point that coherent wave patterns or ordered waves could be induced by the local perturbation such as a localized inhomogeneity. However, they treat quite different contexts. Reference [11] deals with the oscillatory media in the vicinity of Hopf-bifurcation while this current work deal with excitable media. The pattern, whether spiral waves or target waves, is finally selected does not only depend on the absolute value of the frequency but also on the phase difference between Re W and Im W [W is the complex amplitude and Re W (Im W) denotes the real (imaginary) part of W] in the framework of the CGLE [11]. Once the value of the frequency and the phase difference (ahead or behind of) is known, the pattern which is selected is determined. So, the inhomogeneity with the exactly same property will give rise to the same kind of pattern in [11]. Nevertheless, for excitable media we find the exactly same inhomogeneity is possible to induce both spiral and target wave patterns for some situations.

Our work though has been performed on the equations modeling chemical reaction, the result that a completely irregular state can be altered to a well-defined spatiotemporal state, might propose potential applications in biological systems. For instance, in the context of synchronization, this is a simple way to entrain the dynamical systems through locally varying one suitable parameter of the system. By this way, waves can propagate throughout the biological tissue successfully.

Our present results seem possible to be observed in the experiments such as the CO oxidation on Pt(110) or the light-sensitive BZ reaction. As we know, in both system spiral turbulence has been observed. What is more, the parameters used in our model (a,b,ϵ) have a counterpart (p_{CO},p_{O_2},T) in the experiment of the CO oxidation on Pt(110) [30]. Though it seems difficult to locally modulate the pressure of oxygen under experiment conditions, it is possible to construct artificially "inhomogeneity" or "defect" by imposing different metal components onto Pt(110) surface using microelectronics fabrication techniques [31–34]. Modeling "inhomogeneity" is essential regarded as varying locally the kinetics parameter b in the reduced version of the model [33,34]. This situation is similar to what we did in the present work. Additionally, a localized inhomogeneity might also be realized experimentally in the oscillatory CO oxidation on Pt(110) by means of focused laser light [17,39,40].

In summary, we have investigated the possible effects of a localized inhomogeneity (oscillatory or stationary) on the spatiotemporal chaotic state in a chemical excitable medium. We have found that coherent wave patterns such as spiral wave including single-armed and multiple armed, and target wave patterns could be induced and sustained by the localized inhomogeneity. After a transient period, these kinds of coherent wave patterns suppress the previously existing turbulent waves. The formation of spiral wave patterns can be regarded as result from the perturbation of a localized spiral by the inhomogeneity while the detailed way of the inhomogeneity with different properties to sustain the coherent wave patterns seems a little different. At last, we hope our results could be reproduced in the experiment such as the CO oxidation on Pt(110) or the light-sensitive BZ reaction, which will make our work more interesting.

ACKNOWLEDGMENTS

This work was supported by the National Natural Science Foundation of China. We would like to thank Xiaoyi He for useful discussions.

[1] *Chemical Waves and Patterns*, edited by R. Kapral and K. Showalter (Kluwer, Dordrecht, The Netherlands, 1995).
[2] A. T. Winfree, *When Time Breaks Down* (Princeton, Princeton, NJ, 1987).
[3] Q. Ouyang and Flesselles, Nature (London) **379**, 143 (1996).
[4] M. Kim, M. Bertram, M. Pollmann, A. von Oertzen, A. S. Mikhailov, H. H. Rotermund, and G. Ertl, Science **292**, 1357 (2001).
[5] M. Bär and M. Eiswirth, Phys. Rev. E **48**, R1635 (1993).
[6] S. Alonso, F. Sagues, and A. S. Mikhailov, Science **299**, 1722 (2003).
[7] N. J. Wu, H. Zhang, H. P. Ying, Z. Cao, and G. Hu, Phys. Rev. E **73**, 060901(R) (2006).
[8] I. Aranson, H. Levine, and L. Tsimring, Phys. Rev. Lett. **72**, 2561 (1994).
[9] H. Zhang, Z. Cao, N. J. Wu, H. P. Ying, and G. Hu, Phys. Rev. Lett. **94**, 188301 (2005).
[10] H. Zhang, B. Hu, and G. Hu, Phys. Rev. E **68**, 026134 (2003).
[11] X. He, H. Zhang, B. Hu, Z. Cao, B. Zheng, and G. Hu, New J. Phys. **9**, 66 (2007).
[12] G. Baier, S. Sahle, J. P. Chen, and A. A. Hoff, J. Chem. Phys. **110**, 3251 (1999).
[13] R. Zhang, L. Yang, A. M. Zhabotinsky, and I. R. Epstein, Phys. Rev. E **76**, 016201 (2007).
[14] M. Jiang, X. Wang, Q. Ouyang, and H. Zhang, Phys. Rev. E **69**, 056202 (2004).
[15] G. Y. Yuan, S. G. Chen, and S. P. Yang, Eur. Phys. J. B **58**, 331 (2007).
[16] J. Gao and M. Zhan, Phys. Lett. A **371**, 96 (2007).
[17] C. Punckt, M. Stich, C. Beta, and H. H. Rotermund, Phys. Rev. E **77**, 046222 (2008).
[18] K. Agladze, M. W. Kay, V. Krinsky, and N. Sarvazyan, Am. J. Physiol. Heart Circ. Physiol. **293**, H503 (2007).
[19] A. N. Zaikin and A. M. Zhabotinsky, Nature (London) **225**, 535 (1970).
[20] G. Ertl, Science **254**, 1750 (1991).
[21] J. M. Davidenko, A. V. Perstov, R. Salomonsz, W. Baxter, and J. Jalife, Nature (London) **355**, 349 (1992).
[22] F. Xie, Z. Qu, and A. Garfinkel, Phys. Rev. E **58**, 6355 (1998).
[23] O. Steinbock and S. C. Müller, Phys. Rev. E **47**, 1506 (1993).
[24] X. Zou, H. Levine, and D. A. Kessler, Phys. Rev. E **47**, R800 (1993).
[25] A. P. Muñuzuri, V. Perez-Muñuzuri, and V. Perez-Villar, Phys. Rev. E **58**, R2689 (1998).
[26] Y. Q. Fu, H. Zhang, Z. Cao, B. Zheng, and G. Hu, Phys. Rev. E **72**, 046206 (2005).
[27] A. Pumir, V. Nikolski, M. Horning, A. Isomura, K. Agladze, K. Yoshikawa, R. Gilmour, E. Bodenschatz, and V. Krinsky, Phys. Rev. Lett. **99**, 208101 (2007).
[28] B. Hu and H. Zhang, Int. J. Mod. Phys. B **17**, 3988 (2003).
[29] T. K. Shajahan, S. Sinha, and R. Pandit, Phys. Rev. E **75**, 011929 (2007).
[30] M. Bär, N. Gottschalk, M. Eiswirth, and G. Ertl, J. Chem. Phys. **100**, 1202 (1994).
[31] M. D. Graham, I. G. Kevrekidis, K. Asakura, J. Lauterbach, K. Krischer, H. H. Rotermund, and G. Ertl, Science **264**, 80 (1994).
[32] M. Pollmann, H. H. Rotermund, G. Ertl, X. Li, and I. G. Kevrekidis, Phys. Rev. Lett. **86**, 6038 (2001).
[33] M. Bär, I. G. Kevrekidis, H. H. Rotermund, and G. Ertl, Phys. Rev. E **52**, R5739 (1995).
[34] M. Bär, A. K. Bangia, I. G. Kevrekidis, G. Haas, H. H. Rotermund, and G. Ertl, J. Phys. Chem. **100**, 19106 (1996).
[35] V. I. Krinsky and K. I. Agladze, Physica D **8**, 50 (1983).
[36] M. Stich and A. S. Mikhailov, Physica D **215**, 38 (2006).
[37] V. Petrov, Q. Ouyang, G. Li, and H. L. Swinney, J. Phys. Chem. **100**, 18992 (1996).
[38] B. W. Li, H. Zhang, H. P. Ying, W. Q. Chen, and G. Hu, Phys. Rev. E **77**, 056207 (2008).
[39] J. Wolff, A. G. Papathanasiou, I. G. Kevrekidis, H. H. Rotermund, and G. Ertl, Science **294**, 134 (2001).
[40] J. Wolff, M. Stich, C. Beta, and H. H. Rotermund, J. Phys. Chem. B **108**, 14282 (2004).